International Journal of Industrial Ergonomics 53 (2016) 27–36

Contents lists available at ScienceDirect

International Journal of Industrial Ergonomics

journal homepage: www.elsevier.com/locate/ergon

Anthropometric body modeling based on orthogonal-view images

Xiaojing Zhou [a, *], Jinxiang Chen [b], Guohua Chen [c], Zhengxu Zhao [d], Yong Zhao [e]

[a] School of Instrument Science and Engineering, Southeast University, Nanjing 210096, PR China
[b] School of Civil Engineering, Southeast University, Nanjing 210096, PR China
[c] School of Information Science and Engineering, Southeast University, Nanjing 210096, PR China
[d] School of Computing and Informatics, Shijiazhuang Tiedao University, Shijiazhang 050043, PR China
[e] System Consulting Dept., Aimnext Inc., Minato-Ku, Tokyo 105-0013, Japan

ARTICLE INFO

Article history:
Received 5 December 2014
Received in revised form
2 October 2015
Accepted 26 October 2015
Available online xxx

Keywords:
Anthropometry
Digital human models (DHM)
Free-form deformation (FFD)
Photograph
Model reconstruction

ABSTRACT

This paper presents an efficient and convenient method for creating an anthropometric model of a real person. First, 3D surface body models based on orthogonal-view photographs are reconstructed, and then skeletal systems for the reconstructed models are matched. A total of 26 anthropometric data items are measured using the surface and skeletal models. Some anthropometric data are measured directly on the deformed surface models, whereas others are estimated from the matched skeletal systems by kinematic analysis. A comparison of the anthropometric data from the reconstructed model with data from the corresponding real person demonstrates that the methodology proposed in this paper has high efficiency and precision. These models will satisfy consumer demand for higher product personalization and therefore product comfort, and they are likely to be widely used in future ergonomic research.

Relevance to industry: A convenient and efficient method to create individual anthropometric models is proposed. These models will help people create their own anthropometry databases and satisfy their demand for higher product personalization and therefore product comfort. The industrial applications include mass customization, computer-aided drafting, online custom-made design, and ergonomic evaluation.

1. Introduction

An anthropometric model is a digital human model (DHM) built on anthropometric data measured under defined poses. Such models are used to analyze the ergonomic performance of a proposed product (Duffy, 2009; You and Ryu, 2005). Current ergonomic software packages, such as JACK (Demirel, 2006), ErgoForms (Dreyfuss, 2001) and PeopleSize 2000, are based on statistical descriptions of human variability and lack the ability to build models for specific individuals. With the increasing popularity of ordering custom-made products via online shopping, people are paying more attention to the usability of a product for themselves. Therefore, a single convenient method for creating individual anthropometric models and helping customers measure their own body size has broad applications in the fields of internet shopping, virtual try-on systems, industrial design, and healthcare.

Anthropometry modeling methods are classified from scanners and photographs. Allen et al.(Allen et al., 2002, 2003) created a static and dynamic model using a point cloud and sparse marks with a 3D body scanner. Baek et al. (Baek and Lee, 2012) extracted anthropometric data from a real person using a range scan, deformed the template model using these data, and then reconstructed the 3D detailed model. In the research of Thomassey and Bruniaux, a reverse methodology using scans of a reference body and garment enabled the evaluation of the overall 3D ease of the garment (Thomassey and Bruniaux, 2013).

The 3D whole-body scanning method is the most accurate method for obtaining body shape information, but the technology is highly complex and difficult for the typical customer to understand (Nadadur and Parkinson, 2013). A feasible solution to this problem is for customers to create their own 3D models from 2D photographs. Hilton et al. and Lee et al. reported a robust method for establishing a model of an individual person with orthogonal photographs (Hilton et al., 1999; Lee et al., 2000; Magnenat-Thalmann et al., 2011; Zhu et al., 2013). They extracted the silhouettes from 2D images and deformed the 3D unified models by adding this detailed information. Free-form deformation (FFD) is the deformation algorithm currently used to morph DHMs because

* Corresponding author.
E-mail address: xiaojingzhou@seu.edu.cn (X. Zhou).

http://dx.doi.org/10.1016/j.ergon.2015.10.007
0169-8141/

it can retain the continuity and characteristics of the human body (Kasap and Magnenat-Thalmann, 2007). Zhu et al. (Zhu et al., 2013) adopted a new deformation algorithm-composite triangle (CT) FFD that can minimize distortion and closely resemble the geometrical shape of the control mesh. However, compared to the scanning method, orthogonal modeling has a lower accuracy and lower fidelity of detail simulation (Simmons and Istook, 2003). Therefore, in the present paper, the global and local deformation methods are adopted sequentially to improve accuracy. Our modeling method aims to model a specific person and not a statistical crowd. Then, a skeletal system is matched to each deformed model, and anthropometric data are measured from these models to enable the construction of a large-scale ergonomic database.

2. 3D digital human body modeling

2.1. Defining characteristic points

To determine the relationship between the 2D images and 3D surface model, the characteristic points must first be defined. Consider the frontal view images of the photograph in Fig. 1 as an example, which show binary image processing (Gabarra and Tabbone, 2005) and silhouette extraction. Such images must be taken under the conditions of a simple background, even lighting and form-fitting clothing. The focal plane must be parallel to the coronal or sagittal plane as accurately as possible when taking the front and side photographs.

For 2D body silhouettes, the characteristic points include three types of points: extreme, primary and secondary. There are seven extreme points in the extracted 2D silhouettes: five in the front picture and two in the side picture. These are denoted with triangular symbols in Fig. 2(a) and (b) and are the maximum or minimum points along two axis directions on the 2D silhouettes.

The primary and secondary characteristic points are used to determine the segmentation of the human body. Except for the crotch point, their positions can be determined by referring to the standard body proportion of Chinese adults (GB, 1988). The primary points, denoted with x symbols in Fig. 2(a) and (b), divide the body into six parts: the head, left and right legs (including feet), left and right arms (including hands) and trunk. The secondary characteristic points, denoted with circular symbols, belong to and subdivide one part of body. For example, a leg can be divided into the thigh, calf and foot according to the secondary points. For the trunk, the secondary points define the breadth and depth of the bust, waist and hip in the front and side silhouettes of the body. Because the silhouettes of the arm are surrounded by the body's silhouette in side silhouettes, the secondary points of the arm are limited to the frontal projection.

To obtain the 3D individual model, the method adopted here deforms the template model. The template (Fig. 2(c)) is a surface model composed of triangle meshes and is divided into six parts, similar to Fig. 2(a) and (b). For the convenience of description, the silhouettes (Fig. 1(c)) from the 2D photographs are named $R2$, the silhouettes (Fig. 2(a) and (b)) from the 2D front and side projection of the 3D template are named $T2$, the 3D template model (Fig. 2(c)) is named $T3$, and the final 3D model of the real person is named $R3$.

2.2. Deformation of DHM

2.2.1. Free-form deformation

In 1986, Sederberg and Parry (Sederberg and Parry, 1986) presented the FFD method, which uses the basic concept of embedding the object to be transformed into a frame with many lattices. With the action of the outer forces on the frame but not the object, the control frame produces deformation, and this deformation will pass to the object. FFD has the advantage of maintaining the continuity of closed surfaces after deformation. If l, m and n are the numbers of subdivisions along each of the three directions, S, T and U, $l+1$, $m+1$ and $n+1$ are the numbers of control planes in the three coordinate directions, respectively, and $(l+1)\times(m+1)\times(n+1)$ is the number of control points. As shown in Fig. 3, the lattice is divided into 2 parts in three directions such that $l=m=n=2$. In total, there are 27 control points (black filled circles in Fig. 3).

Mathematically, the FFD is defined in terms of a tensor product tri-variate Bernstein polynomial. To impose a grid of control points P_{ijk} on the parallelepiped, the deformation is specified by moving P_{ijk} from their lattice positions. P_{ijk} can be represented by Equation (1) as follows:

$$P_{ijk} = X_0 + \frac{i}{l}S + \frac{j}{m}T + \frac{K}{n}U \quad (i=0,1,\cdots,l;\quad j=0,1,\cdots m;\quad k=0,1,\cdots n) \tag{1}$$

where X_0 is the original point of the coordinate under axis S, T and U. The deformed position X_d of an arbitrary point X can be evaluated by the Bernstein polynomial B as follows:

$$X_d = \sum_{i=0}^{l}\sum_{j=0}^{m}\sum_{k=0}^{n} B_{i,l}(s)B_{j,m}(t)B_{k,n}(u)P_{ijk} \tag{2}$$

where (s,t,u) is the original normalization coordinate of point X that conforms to the conditions $0<s<1$, $0<t<1$ and $0<u<1$. The Bernstein polynomial can be expanded as

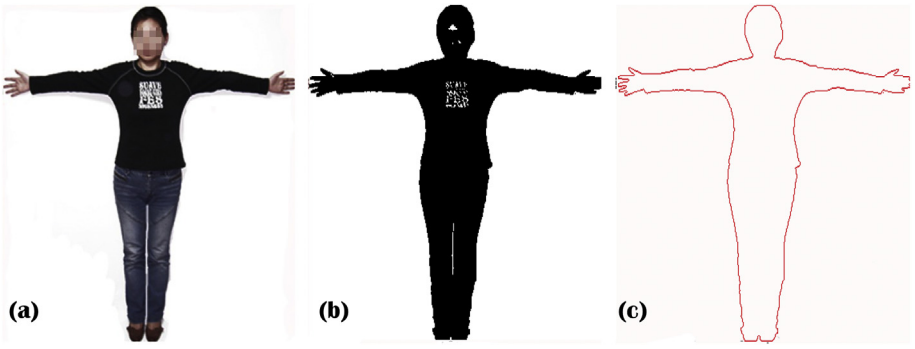

Fig. 1. Extraction of 2D silhouettes. (a) original image, (b) gray-scale image, (c) silhouette image.

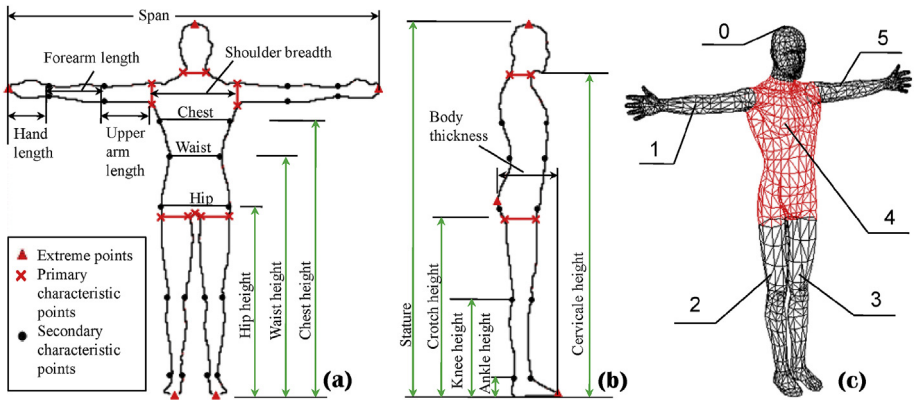

Fig. 2. Characteristic points on body silhouettes and a 3D template model. (a) front projection, (b) side projection, (c) 3D template model (divided into six parts based on primary points: 0– head; 1, 5–right and left arms (including hands); 2, 3 – right and left legs (including feet); 4 – trunk).

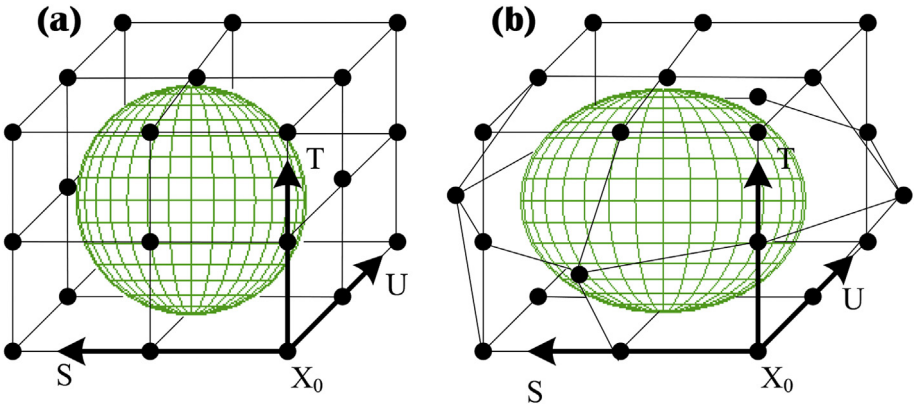

Fig. 3. Free-form deformation. (a) control points of the initial lattice, (b) displaced control points of the final lattice.

$$X_d = \sum_{i=0}^{l} C_l^i s^i (1-s)^{l-i} \left(\sum_{j=0}^{m} C_m^j t^j (1-t)^{m-j} \left(\sum_{k=0}^{n} C_n^k u^k (1-u)^{n-k} P_{ijk} \right) \right) \tag{3}$$

Equation (3) is the deformation equation, which is unique to every FFD. The deformed result is obtained by computing all of the vertexes on the meshes with this equation. To improve the accuracy of the deformation, the FFD of the virtual human model consists of two stages in this paper: global deformation and local deformation. Global deformation builds the control lattices for the entire template model and adjusts the main dimensions, such as stature, span, and length of the legs and arms, to approximate the 2D silhouettes of the real person. Local deformation builds the control lattices for each part of the body and simulates some details of the real body, such as the waist circumference and the length of the upper arm.

2.2.2. Global deformation

As shown in Fig.4, a 3D mesh model is embedded into a control cube. The cube, where $i = 1, j = k = 3$, has 9 lattices and 32 control points. The sequence numbers of these control points are $P_{000} - P_{133}$. The original point $P_{000}(0,0,0)$ is the minimum coordinate of all body points in three directions, and the point $P_{133}(1,1,1)$ is the maximum coordinate. The control point is easy to calculate because the control grid is evenly detached. For example, the coordinate of point P_{121} is (1,2/3,1/3).

When the control points move, arbitrary points of the model

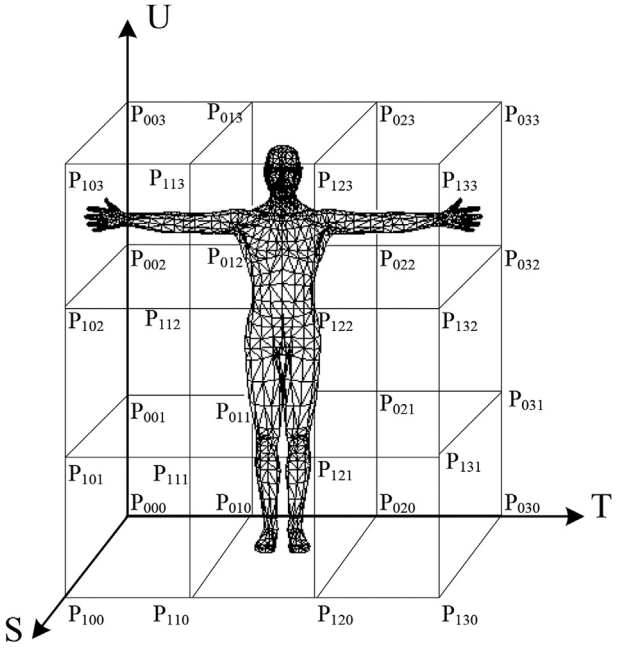

Fig. 4. Control lattices for global deformation (P_{000}–P_{133} are 32 control points using for FFD).

will consequently deform. The displacement of the control points can be arbitrary or restrictive. As for the global deformation and local deformation, the constraint conditions of the control points are different. Once the movement of the control points is determined, the deformation equation can be solved. In this paper, on the condition that the position of the characteristic points in the deformed model must coincide with the corresponding characteristic points in the silhouettes of the photographs, the positions of the control points after deformation are reversely deduced.

The purpose of global deformation is to superimpose the 3D template onto the 2D silhouettes from photographs at the position of the extreme points and primary characteristic points. Thus, the main dimensions of the newly deformed 3D model, such as stature, arm length, shoulder spread and crotch height, are similar to those of the real person. Considering that the anthropometric measurement planes of body dimensions are defined as horizontal and vertical, the global deformation maintains this relationship between the control planes. Therefore, the control grid will be similarly transferred. The result of the deformation is that the control points in a given plane are still control points in the other given plane. Suppose that after removal, the coordinates of 32 control points $P_{ijk}(i = 0–1, j = 0–3, k = 0–3)$ are expressed as (s_p,t_p,u_p). To ensure that control points move in parallel, the coordinates can be represented as follows:

$$\begin{cases} s_p = \begin{cases} 0 & i = 0 \\ S_i & i = 1 \end{cases} \\ t_p = \begin{cases} 0 & j = 0 \\ T_j & j = 1,2,3 \end{cases} \\ u_p = \begin{cases} 0 & k = 0 \\ U_k & k = 1,2,3 \end{cases} \end{cases} \tag{4}$$

where $S_i(i = 1)$, $T_j(j = 1–3)$, and $U_k(k = 1–3)$ are the parameters that determine the position of the control points. Because the lattice is even, the initial values of these parameters before global deformation are

$$\begin{cases} S_i = 1 & i = 1 \\ T_j = j/3 & j = 1,2,3 \\ U_k = k/3 & k = 1,2,3 \end{cases} \tag{5}$$

Suppose that $X_d(s_d,t_d,u_d)$ is the coordinate of arbitrary vertexes $X(s,t,u)$ in meshes after deformation. To substitute Equation (4) into the FFD deformation formula (3), the transformation from X to X_d can be deduced as in Equation (6):

$$\begin{cases} s_d = S_1 s \\ t_d = 3T_1 t(1-t)^2 + 3T_2 t^2(1-t) + T_3 t^3 \\ u_d = 3U_1 u(1-u)^2 + 3U_2 u^2(1-u) + U_3 u^3 \end{cases} \tag{6}$$

To obtain the final deformation equation as in (6), the parameters $S_i(i = 1)$, $T_j(j = 1–3)$, and $U_k(k = 1–3)$ must be solved. The parameters in Equation (6) can be solved by substituting the coordinates of the extreme points and primary characteristic points in $T2$ to X and substituting those in $R2$ to X_d. By imposing the global deformation to all of the vertexes in $T3$, the 3D surface model of the real person $R3$ is obtained, as shown in Fig. 5(h–j). Fig. 5 shows that the deformed model has the same approximate dimensions of span, body thickness, and arm and leg length as the 2D silhouettes of the real human.

2.2.3. Local deformation

To have the new 3D model approach the shape of the real person, details must be adjusted after global deformation. First, each part of the body, arm, leg or trunk can be viewed as corresponding to a cylinder. Then, the control volume of each part is divided into layers along the primary axis direction and divided equally along the other two coordinate axis directions as shown in Fig. 6(a). The control points in the 0th layer, nth layer and primary axis are fixed, which ensure that the mesh surfaces between two body parts do not produce any rupture or superposition. Along the primary axis, the control points of a layer remain in the same layer after deformation. This process, called local deformation, is shown in Fig. 6.

The initial values of the control points $P_{ijk}(s_p,t_p,u_p)$ before local deformation are

$$\begin{cases} s_p = j/2 & j = 0,1,2 \\ t_p = k/2 & k = 0,1,2 \\ u_p = i/n & 0 \le i \le n \end{cases} \tag{7}$$

In terms of the features of the local deformation, the position of the control points in the 0th layer and nth layer are unchanged and can be calculated by Equation (7). However, the coordinates of the control points in other layers, i.e., $1 \le i \le n-1$, are expressed as follows:

$$\begin{cases} s_p = \begin{cases} S_{i1} & j = 0 \\ 1/2 & j = 1 \\ S_{i2} & j = 2 \end{cases} \\ t_p = \begin{cases} T_{i1} & k = 0 \\ 1/2 & k = 1 \\ T_{i2} & k = 2 \end{cases} \\ u_p = U_i \end{cases} \tag{8}$$

where S_{i1}, S_{i2}, T_{i1}, and T_{i2} are undetermined parameters in the local deformation equation as shown in Fig. 6(b). Similarly, substituting Equation (8) into Equation (3), the local deformation equation is obtained as follows:

$$\begin{cases} s_d = \frac{1}{2}B_{1,2}(s) + B_{2,2}(s) + \sum_{i=1}^{n-1} B_{i,n}(u)\left[B_{0,2}(s)S_{i1} + B_{2,2}(s)(S_{i2}-1)\right] \\ t_d = \frac{1}{2}B_{1,2}(t) + B_{2,2}(t) + \sum_{i=1}^{n-1} B_{i,n}(u)\left[B_{0,2}(t)T_{i1} + B_{2,2}(t)(T_{i2}-1)\right] \\ u_d = \sum_{i=1}^{n-1} B_{i,n}(u)U_i + B_{n,n}(u) \end{cases} \tag{9}$$

Considering the trunk as an example, the dimensions of the trunk include the measurements of the chest, waist and hips and their positions. If $n = 4$, there are $5 \times 3 \times 3 = 45$ control points and $27 - 3 = 24$ points in the three middle layers (except the central points) that are changeable.

To solve the parameters in the equations, the positions of some secondary points must be calculated in $T2$ and $R2$. After substituting the coordinates of these secondary points into Equation (9), the local deformation is uniquely determined. Fig. 7 presents the original state and the result of the local deformation of the trunk. The reconstructed surface model (Fig. 8) is created by combining the global and local deformations; the shape and main body dimensions are approximate to the real person's shape and dimensions.

3. Anthropometric measurement in the DHM

Anthropometric measurement using the DHM is different than measurement on a real human body. Basic anthropometric data include measurements collected while the subject stands and sits, measurements on specific body segments (such as hands, feet and head) and functional measurements (GB, 2010; ISO, 2008).

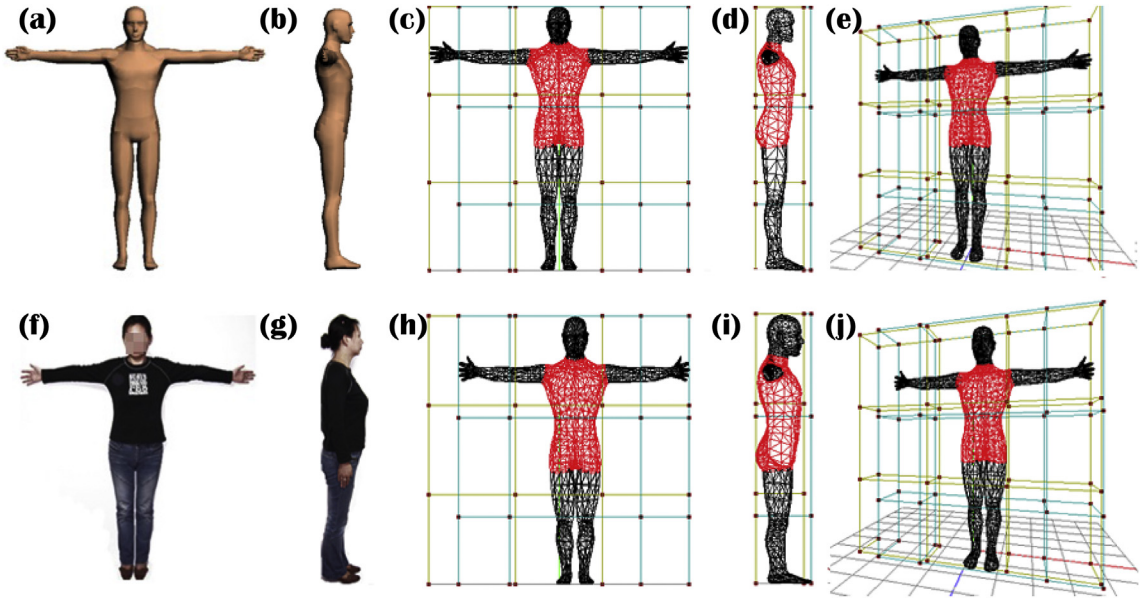

Fig. 5. Results of global deformation. (a), (b) orthogonal-view images before deformation, (c)–(e) 3D template model, (f), (g) orthogonal-view images after deformation, (h)–(j) 3D deformed model.

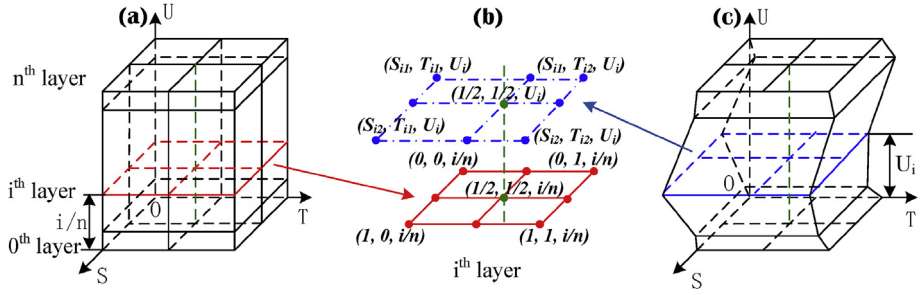

Fig. 6. Lattices for local deformation. (a) before local deformation, (b) change of control points in the ith layer (filled circles along solid lines are the control points before deformation, whereas those along dot-dash lines are the control points after deformation), (c) after local deformation.

However, due to the limitation of the posture in the photograph, when a subject stands with two arms stretched out sideways, only some basic data can be measured on the above deformed surface models. Other anthropometric data are extracted from the matched skeletal models as described below.

3.1. Matching skeletal system

By matching the skeletal system to our models, the initial posture can be transferred to a new measurement posture from which we can obtain new anthropometric data. For example, to measure vertical grip reach, the upper limb is rotated upward around the shoulder to the vertical orientation. Then, the data are extracted from this position.

3.1.1. Standard skeletal system

The skeletal system applied in this paper, shown in Fig. 9, is based on the theory of anthropometry combined with the FFD algorithm. This skeleton is linked to 20 critical points, numbered 0 through 19, with 5 points being the extreme end points and the remainder being joint points that serve as the central points of some of the loops in Fig. 9(c). These central points include the primary and secondary characteristic points.

3.1.2. Matching process

Fig. 10 illustrates the four main steps of matching the skeletal system. The key to matching skeletons is to find the joint points. To compute the position of the joint, the boundary loop (in which all points belong to two body parts at the same time) must be extracted from the meshes. The arithmetic of searching the boundary is based on the fact that for one body part, the line representing the boundary belongs only to one triangle, but the line not on the boundary is shared by two triangles. According to this principle, ergodical arithmetic is adopted to gain the boundary. The joint point is the geometrical center of all points in the boundary loop. As shown in Fig. 9(a), the joint points 1, 3, 4, 5 and 6 are obtained by this arithmetic.

Other joint points cannot be computed by ergodical arithmetic because they are inside one part. This paper presents a method to evaluate the intersecting loops between the plane and triangle meshes to find the joint points. Considering the right leg as an example, the plane parallel to the ground at the height of the ankle and knee can be obtained first. Then, computing the intersecting points between the plane and triangle meshes of the leg and averaging their coordinates, the joint points on the ankle and knee, marked as 11and 13 in Fig. 9, can be determined. All of the boundary and intersecting loops and their central points are indicated in Fig. 10(a) and (b).

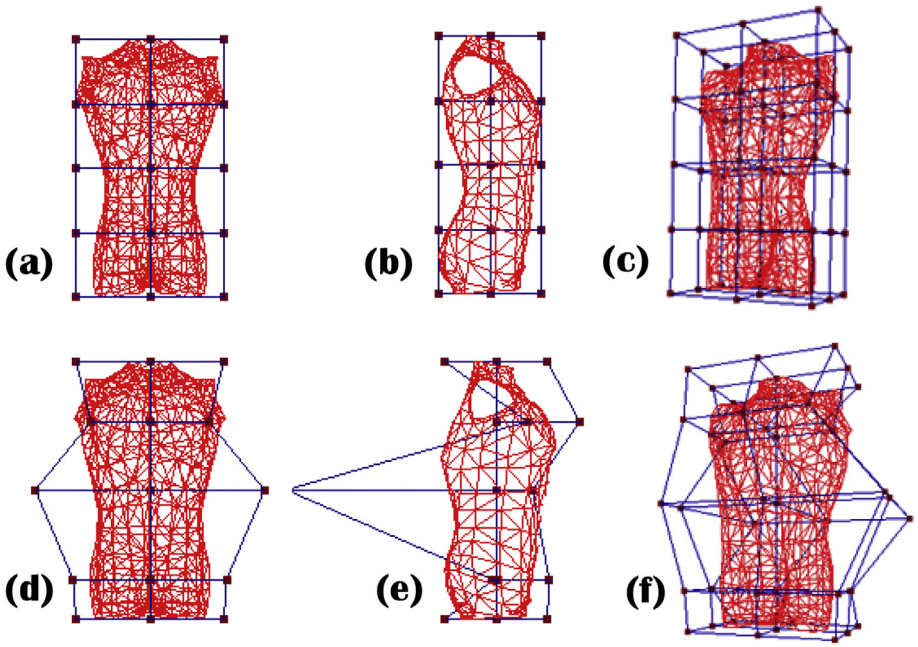

Fig. 7. Results of local deformation of the trunk. (a)–(c) before deformation, (d)–(f) after deformation.

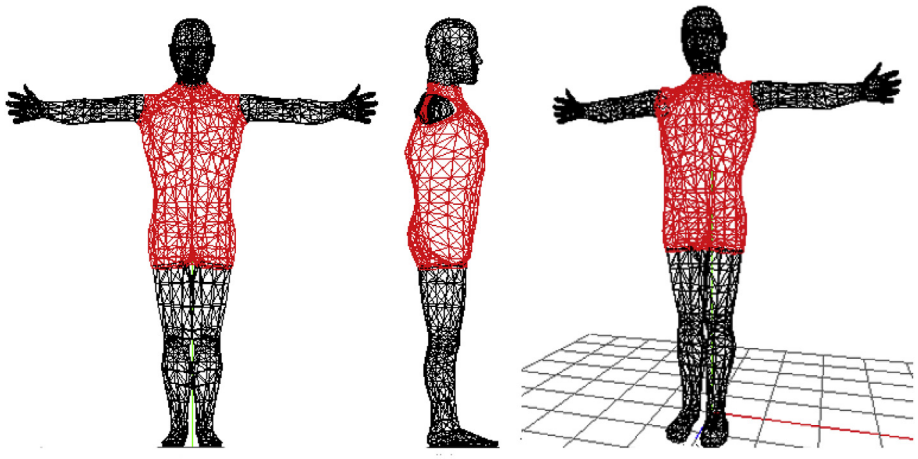

Fig. 8. Final results of the 3D surface model after global and local FFD.

The end points, such as points 15, 16, 17, 18 and 19 in Fig. 9, can be easily obtained by computing the extreme points. To link all of the joint and extreme points, the skeletal system matching the deformed surface model is created, as shown in Fig. 10(c) and (d). Because the skeletal system is created based on *R3*, the bones in this system have similar dimensions to those of the person.

3.2. Anthropometric measurement method

After reconstructing the model and matching its skeletal system, the anthropometric measurement can be executed using the model of the real person instead of the person directly. Here, we extract anthropometric data from the surface model and the skeleton model. This technique for building an anthropometric database is convenient for customized online shopping and expands current databases.

All 26 items of anthropometric data are measured in this paper. Because the anthropometric measurement items and their definitions vary among countries, Table 1 lists the references of these dimensions. Most items refer to international or national standards, including ISO 7250-2008 (ISO, 2008), JIS Z 8500-2002 (JIS, 2002) and GB/T 5703-2010 (GB, 2010), and some items come from the reference book entitled "Body space: anthropometry, ergonomics, and the design of work" (Pheasant and Haslegrave, 2006). The other items lacking any indicated reference are the complements of current standards.

3.2.1. Anthropometric measurement on 3D surface models

The measurements obtained directly from 3D surface models are classified into three categories: height dimensions, such as neck height and knee height; breadth dimensions, such as span and upper limb length; and dimensions relating to circumference, such as chest circumference and bust (chest) breadth. We assumed that the stature of the model is the same as that of the real person, and other sizes in the model are computed based on this supposition.

The height and breath dimensions have been computed in the

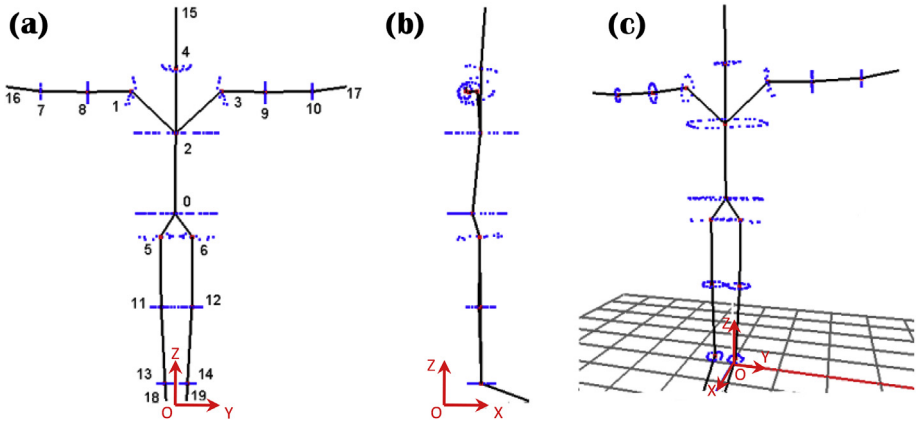

Fig. 9. Standard skeletal system. (a) front projection, (b) side projection, (c) 3D skeletal system (0 – hips; 1 – right shoulder; 2 – chest; 3 – left shoulder; 4 – neck; 5 – right coxa; 6 – left coxa; 7 – right wrist; 8 – right elbow; 9 – left elbow; 10 – left wrist; 11 – right knee; 12 – left knee; 13 – right ankle; 14 – left ankle; 15 – head top; 16 – right middle fingertip; 17 – left middle fingertip; 18 – right toe tip; 19 – left toe tip).

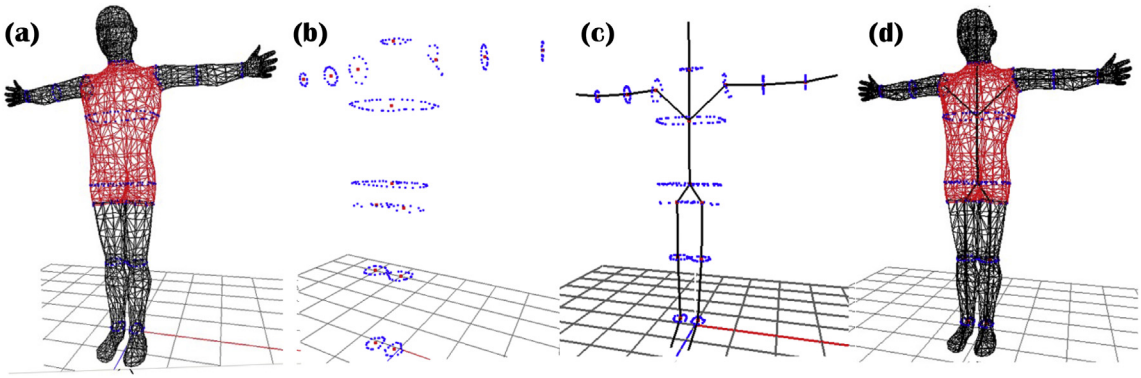

Fig. 10. Steps for matching the skeletal system. (a) intersecting loops, (b) joint points, (c) skeletal system, (d) skeleton model.

Table 1
Anthropometric measurement items and reference standards.

Classification	Dimension	Reference standard
Height	1. Stature	ISO 7205-1:2008 4.1.2; JIS Z 8500:2002 5.2.2; GB/T 5703-2010 4.1.2
	2. Cervicale height	JIS Z 8500:2002 5.2.4; GB/T 5703-2010 4.2.3
	3. Chest height	
	4. Waist height	
	5. Hip height	Body Space 2.5.5
	6. Crotch height	ISO 7205-1:2008 4.1.7; JIS Z 8500:2002 5.2.15; GB/T 5703-2010 4.1.7
	7. Tibiale (knee) height	ISO 7205-1:2008 4.1.8; JIS Z 8500:2002 5.2.16
	8. Ankle (foot) height	
Length	9. Span	JIS Z 8500:2002 5.2.17
	10. Shoulder breadth[a]	ISO 7205-1:2008 4.2.8; JIS Z 8500:2002 5.2.30; GB/T 5703-2010 4.2.8
	11. Upperarm length	JIS Z 8500:2002 5.2.19
	12. Forearm length	JIS Z 8500:2002 5.2.20
	13. Hand length	ISO 7205-1:2008 4.3.1; JIS Z 8500:2002 5.2.43
Circumference	14. Chest circumference	ISO 7205-1:2008 4.4.9; JIS Z 8500:2002 5.2.43
	15. Chest breadth	ISO 7205-1:2008 4.1.11; JIS Z 8500:2002 5.2.32; GB/T 5703-2010 4.1.11
	16. Chest depth	JIS Z 8500:2002 5.2.37; GB/T 5703-2010 4.1.9
	17. Waist circumference	ISO 7205-1:2008 4.4.10; JIS Z 8500:2002 5.2.44
	18. Waist breadth	
	19. Waist depth	
	20. Hip circumference	
	21. Hip breadth	ISO 7205-1:2008 4.1.12; JIS Z 8500:2002 5.2.36; GB/T 5703-2010 4.1.12
	22. Hip depth	
Other	23. Dactylion height	JIS Z 8500:2002 5.2.9
	24. Dactylion height, over head	JIS Z 8500:2002 5.2.12
	25. Arm reach from back	JIS Z 8500:2002 5.2.24
	26. Elbow height, standing	Body space 2.5.4

[a] In the reference standard, the item is measured when the subject is sitting, but in our paper, it is measured when the subject is standing.

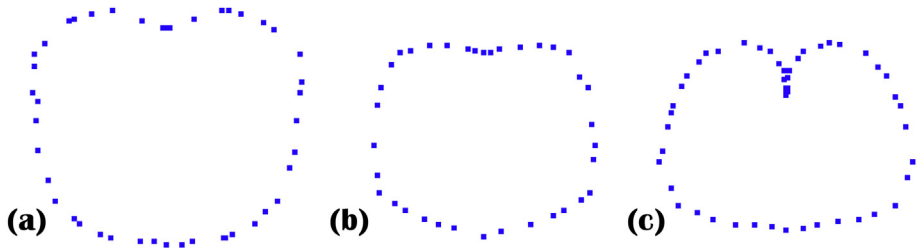

Fig. 11. Bust, waist and hip circumference of reconstructed model. (a) bust circumference, (b) waist circumference, (c) hip circumference.

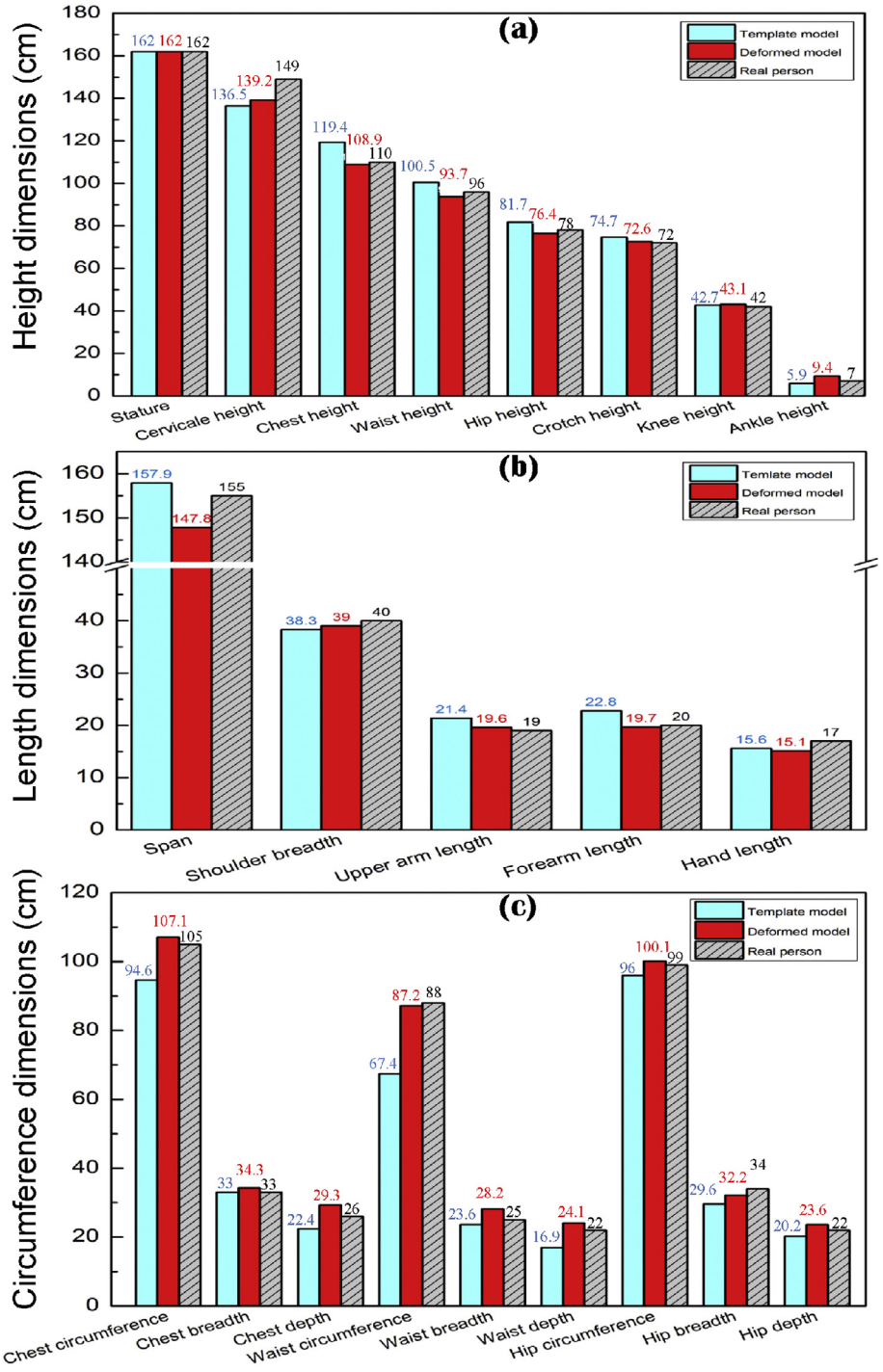

Fig. 12. Anthropometric data measured in the 3D surface model. (a) height dimensions, (b) length dimensions, (c) circumference dimensions.

process of extracting characteristic points in global and local deformation. Dimensions relating to circumference are obtained at the same time as the loops in Fig. 10(b) are computed for joint points. The perimeter of the loop can be viewed as the circumference. For example, the loops at the bust, waist and hip positions are diagramed in Fig. 11; the perimeters are considered to approximate the bust, waist and hip circumferences. Fig. 12 compares the anthropometric dimensions computed in *T3* and *R3* with the actual values measured on the real person. There are a total of 22 items: 8 items with height dimensions, presented in Fig. 12(a); 5 items with length dimensions, presented in Fig. 12(b); and 9 items related to circumference dimensions, presented in Fig. 12(c). The anthropometric dimensions of R3 are closer to those of the real person than are those of T3 except for knee height, ankle height, span, hand length and waist breadth. For the length and circumference dimensions, the average errors of T3 and R3 decrease from 8.20% to 4.60% and from 11.12% to 6.17%, respectively.

3.2.2. Anthropometric measurement on 3D skeletal models

The other anthropometric data, such as sitting measurements and functional measurements, must be measured using the matching skeletal system. By kinematic analysis of the skeleton and joint system, the static model is changed to other measuring postures to extract the dimensions.

Suppose that the coordinate of 20 nodes in the skeletal system is $V_n(x_n,y_n,z_n)$ in Fig. 9(a), where $n = 0–19$, and the coordinate system is shown in Fig. 9. Suppose that the shoulder joint V_3 is the center of rotation. When the left arm $V_3–V_9–V_{10}–V_{17}$ is rotated 90° upward, the dactylion height overhead can be measured from the floor to the dactylion. Similarly, the dactylion height and arm grip reach are obtained by rotating the arm 90° downward and forward, respectively. Additional measurements, such as elbow height (standing) and the zones of convenient reach, can be estimated using the skeletal model. Some comparative results of these anthropometric measurements are shown in Fig. 13.

Figs. 12 and 13 show that the anthropometric dimensions obtained from the deformed model are close to those of the real person but that there remains some error relative to the actual values. The reasons for this error include the following. First, the segmentation of the lattices is not sufficiently fine. For example, the lattices in the global deformation are $1 \times 3 \times 3$, thereby introducing error. Greater subdivision improves the accuracy. Second, due to dimension distortion caused by the shooting angle, the photographs are not an absolute orthogonal projection; thus, the dimensions for the hands, feet and head include some error. The methodology described here can also be used for these measurements, but their photographs of these regions must be taken individually at close range. It is believed that these problems will be solved by the use of greater subdivision and close-range photography. Thus, the method proposed in the paper is convenient, rapid and highly precise but also has considerable development potential.

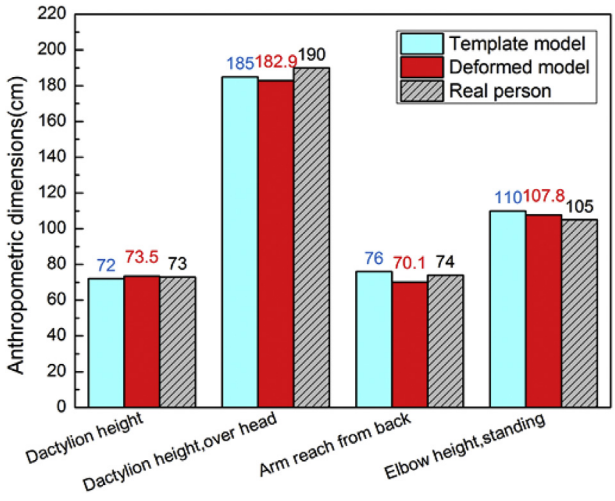

Fig. 13. Anthropometric data measured in 3D skeletal model.

In summary, replacing an expensive scanner with a basic camera and using the information collected from photographs, a 3D individual digital model can be created quickly. First, as input, our system requires one front photograph and one side photograph of a subject in form-fitting clothing. The stature and gender of the subject must be input into the system. Then, silhouette extraction, model deformation and matching skeleton systems are automatically completed with our method. Finally, an anthropometric database including 26 items of dimensions and a 3D model of the subject can be outputted from our system. Compared with the method for building anthropometric databases by scanning the body and analyzing point cloud data (Allen et al., 2002; Baek and Lee, 2012), this method is simpler and more feasible for use by ordinary people.

Many applications of these methods can be found in the ergonomics field, such as in virtual fitting systems, custom-made product designs, the computer-aided drafting clothing industry and healthcare services. Customers can create their own databases and upload models when online shopping or using a made-to-measure service. The designer and manufacturer can style and produce unique 'John's suits' or 'Alice's foot-stool' matching based on the individual's own anthropometric model.

4. Conclusion

In this paper, 3D individual models are created from orthogonal-view images of a real person, from which anthropometric data are collected and computed in a short cycle. The main results of this paper include the following:

1) A new 3D individual body model is reconstructed by extracting silhouettes from orthogonal-view images of a real person, defining the characteristic points, and executing FFD to a given template model. As a result of matching the skeletal system with a surface model, the shapes and skeletal dimensions of the final model are similar to those of the real person.
2) A total of 26 anthropometric data items are measured with the surface and skeletal models. By comparing the anthropometric data from the reconstructed model with those from the corresponding real person, the methodology proposed in this paper resulted in high efficiency and precision and can be widely used in ergonomic research.
3) The paper proposes a new method that enables anyone to create his or her own anthropometric model without relying on current statistical anthropometric databases. This method eliminates the need for anthropometric measurements to be executed by professional organizations and lays the foundation for creating new, networked, large-scale anthropometry databases.

References

Allen, B., Curless, B., Popovi, Z., 2002. Articulated body deformation from range scan data. In: Proceedings 29th Annual Conf. Computer Graphics and Interactive Techniques. ACM. Texas, San Antonio, pp. 612–619.
Allen, B., Curless, B., Popovi, Z., 2003. The space of human body shapes: reconstruction and parameterization from range scans. ACM Trans. Graph. (TOG) 22

(3), 587–594.
Baek, S.-Y., Lee, K., 2012. Parametric human body shape modeling framework for human-centered product design. Comput. Aided Des. 44 (1), 56–67.
Demirel, H.O., 2006. USG Tecnomatix Jack5.0 User Manual and Examples.
Dreyfuss, H., 2001. ErgoForms. http://www.ergoforms.com.
Duffy, V.G., 2009. Handbook of Digital Human Modeling: Research for Applied Ergonomics and Human Factors Engineering. CRC Press.
Gabarra, E., Tabbone, A., 2005. Combining global and local threshold to binarize document of images. Pattern Recognit. Image Anal. 3523, 371–378.
GB, 1988. GB10000–88: Human Dimensions of Chinese adults. China State Bureau of Quality and Technical Supervision.
GB, 2010. GB/T 5703–2010: Basic Human Body Measurements for Technological Design-Part 1: Body Measurement Definitions and Landmarks. China State Bureau of Quality and Technical Supervision.
Hilton, A., Beresford, D., Gentils, T., Smith, R., Sun, W., 1999. Virtual people: capturing human models to populate virtual worlds. Citeseer 174–185.
ISO, 2008. ISO 7250-1: Basic Human Body Measurements for Technological Design – Part 1: Body Measurement Definitions and Landmarks. ISO Copyright Office, Geneva, Switzerland.
JIS, 2002. Ergonomics-basic Human Body Measurements for Technological Design. Japanese Standards Association.
Kasap, M., Magnenat-Thalmann, N., 2007. Parameterized human body model for real-time applications. In: Cyberworlds, 2007. CW'07. International Conference on. IEEE, pp. 160–167.
Lee, W., Gu, J., Magnenat-Thalmann, N., 2000. Generating animatable 3D virtual humans from photographs. In: Computer Graphics Forum 3. Citeseer, pp. 1–10.
Magnenat-Thalmann, N., Kevelham, B., Volino, P., Kasap, M., Lyard, E., 2011. 3d web-based virtual try on of physically simulated clothes. Comput. Aided Des. Appl. 8 (2), 163–174.
Nadadur, G., Parkinson, M.B., 2013. The role of anthropometry in designing for sustainability. Ergonomics 56 (3), 422–439.
Pheasant, S.T., Haslegrave, C.M., 2006. Bodyspace: anthropometry, ergonomics, and the design of work. CRC Press.
Sederberg, T., Parry, S., 1986. Free-form deformation of solid geometric models. ACM Siggraph Comput. Graph. 20 (4), 151–160.
Simmons, K.P., Istook, C.L., 2003. Body measurement techniques: comparing 3D body-scanning and anthropometric methods for apparel applications. J. Fash. Mark. Manag. 7 (3), 306–332.
Thomassey, S., Bruniaux, P., 2013. A template of ease allowance for garments based on a 3D reverse methodology. Int. J. Ind. Ergonomics 43 (5), 406–416.
You, H., Ryu, T., 2005. Development of a hierarchical estimation method for anthropometric variables. Int. J. Industrial Ergon. 35 (4), 331–343.
Zhu, S., Mok, P.Y., Kwok, Y.L., 2013. An efficient human model customization method based on orthogonal-view monocular photos. Comput. Aided Des. 45 (11), 1314–1332.